Human–Robot Role Arbitration via Differential Game Theory

Paolo Franceschi[ID], Nicola Pedrocchi[ID], and Manuel Beschi[ID], *Member, IEEE*

Abstract— The industry needs controllers that allow smooth and natural physical Human-Robot Interaction (pHRI) to make production scenarios more flexible and user-friendly. Within this context, particularly interesting is Role Arbitration, which is the mechanism that assigns the role of the leader to either the human or the robot. This paper investigates Game-Theory (GT) to model pHRI, and specifically, Cooperative Game Theory (CGT) and Non-Cooperative Game Theory (NCGT) are considered. This work proposes a possible solution to the Role Arbitration problem and defines a Role Arbitration framework based on differential game theory to allow pHRI. The proposed method can allow trajectory deformation according to human will, avoiding reaching dangerous situations such as collisions with environmental features, robot joints and workspace limits, and possibly safety constraints. Three sets of experiments are proposed to evaluate different situations and compared with two other standard methods for pHRI, the Impedance Control, and the Manual Guidance. Experiments show that with our Role Arbitration method, different situations can be handled safely and smoothly with a low human effort. In particular, the performances of the IMP and MG vary according to the task. In some cases, MG performs well, and IMP does not. In some others, IMP performs excellently, and MG does not. The proposed Role Arbitration controller performs well in all the cases, showing its superiority and generality. The proposed method generally requires less force and ensures better accuracy in performing all tasks than standard controllers.

Note to Practitioners—This work presents a method that allows role arbitration for physical Human-Robot Interaction, motivated by the need to adjust the role of leader/follower in a shared task according to the specific phase of the task or the knowledge of one of the two agents. This method suits applications such as object co-transportation, which requires final precise positioning but allows some trajectory deformation on the fly. It can also handle situations where the carried obstacle occludes human sight, and

the robot helps the human to avoid possible environmental obstacles and position the objects at the target pose precisely. Currently, this method does not consider external contact, which is likely to arise in many situations. Future studies will investigate the modeling and detection of external contacts to include them in the interaction models this work addresses.

Index Terms—Physical human–robot interaction, role arbitration, differential game theory.

I. INTRODUCTION

HUMAN-ROBOT Interaction (HRI) is the discipline that studies and allows safe and natural interaction between humans and robots [1]. HRI has been growing as a research field in recent years, considering the need for collaborative manufacturing tasks shared between humans and robots within modern factories [2], [3]. In particular, in the field of HRI, Human-Robot Collaboration (HRC) [4] deals with a collaborative approach that allows the robot and the human operator to perform complex tasks together, with direct interaction and coordination [5]. When the interaction and collaboration between humans and robots become physical, we deal with the physical Human-Robot Interaction (pHRI) [6].

A widely used technique to handle pHRI is Impedance/Admittance Control [7], [8]. Moreover, many studies aimed at making the Impedance Control adaptive. Two main methods exist to make Impedance Control adaptive: (i) modify the impedance set-point, and (ii) modify the impedance parameters, *i.e.*, the mass, spring, and damper values. An example of the adaptation of the impedance set-point according to interaction with a human can be found in [9], where optimal trajectory deformation is studied, in [10] that uses a Neural Network to identify the set-point, in [11] with a nonlinear model reference adaptation, in [12] and [13], where a fuzzy logic control updates online the set-point, in [14] the reference trajectory is shaped to ensure it is within the constrained task space, and in [15] with application to teleoperation. Adaptation of the mass-spring-damper parameters is exploited as in [16], [17], [18], and [19]. Recent works aim to modify both impedance parameters and set-point simultaneously. In [20], a hybrid controller allows manual guidance for a robot to assemble an aircraft panel. In [21] and [22], Reinforcement Learning updates the parameters online, while [23] exploits a neural network (NN) to update the desired position and the impedance parameters to maintain stability. In [24], a controller that adapts impedance parameters and velocity is

This article has been accepted for inclusion in a future issue of this journal. Content is final as presented, with the exception of pagination.

2   IEEE TRANSACTIONS ON AUTOMATION SCIENCE AND ENGINEERING

Fig. 1. The typical large object co-manipulation scenario. On one side, a lightweight robot is grasping a large object. The robot cannot hold the object alone because of a limited payload and workspace. Conversely, a human is grasping the same object, with possibly the same problems. In this situation, the robot can guide the human to approach with precision a target pose without exceeding its payload.

proposed, allowing interaction between a human, a robot, and the environment.

The main drawback of the abovementioned approaches is that the robot always represents a passive helper to the human. In contrast, nowadays, many situations require Shared Autonomy (SA) and Shared Control (SC) of the task, leading to the emerging field of *deliberative robotics* [25]. Reference [26] presents a brief survey on SA in pHRI. In this situation, the robot and the human can interact with the controlled system differently, possibly switching roles. Consider that many tasks may require the robot to lead the action away from unwanted situations, taking control over the human in circumstances such as singularity proximity, joint limits, and robot workspace boundaries that may not be visible to a human. In this case, SA relates to Role Arbitration (RA), which can be defined as the mechanism that assigns the control of a task to either the human or the robot [27].

Target applications can be co-manipulation of large objects, such as aeronautical components, as in [20]. In the case of large object manipulation, the precise positioning at the target pose is imposed by assembly tolerances. Still, the connecting trajectory from the picking pose to the target pose can be adjusted [28], [29]. It may also happen that large objects can occlude the human operator's sight, and the robot should prevent collisions with the environment [30]. Figure 1 shows a typical large component co-manipulation.

Another application can involve flexible material co-transportation as in [31] and [32]. Similarly to the previous case, a precise position for the target pose is sometimes needed to match the component's design, such as in composite material draping precisely. Otherwise, structural and aesthetic properties drop. Still, the connecting trajectory can be modified during transportation, with the constraints imposed by the robot limitations and target precision requirement. Other target applications involve the teleoperation of robots, such as in [33], where the human

remotely operates a robotic arm. In that scenario, it is possible that the human cannot see the scene clearly because of occlusions, and the robot should take control [34], or the human guides at a high level and the robot provides trajectory correction [35].

This work wants to investigate Role Arbitration for pHRI to solve such applications. In particular, we rely on Impedance Control. We want to keep the low-level impedance control parameters constant and consider it a given system on which humans and robots can interact. Indeed, making Variable Impedance Control is not always easy and can sometimes be risky and complex [36], possibly involving a deep analysis of the variable impedance of the human arm to guarantee stable controllers [37]. Because Game Theory provides mathematical models of strategic interaction among players, we also want to investigate the Game-Theoretical formulation of the human and the robot interacting with the mass-spring-damper system given by the Impedance Control. Multiple works propose different solutions for the games, possibly involving nonlinear dynamics, that are solved via Reinforcement Learning and Critic Networks [38], [39]. Despite this, with the formulation of the problem proposed in this work (*i.e.,* humans and robots interacting with a virtual linear environment), it is possible to show how the complex interactive problem can be reduced to an easier quadratic problem that can be solved via standard LQR solutions [40] in the cooperative case, and iterative algorithms [41] in the non-cooperative case. This makes implementing the proposed method ready for use and easily solved by standard optimization software.

Therefore, the following subsection is dedicated to the review of the related works regarding (i) Game-Theoretical formulation of human behavior, (ii) Game-Theoretical formulation related to the specific pHRI applications, and (iii) Shared Autonomy and Role Arbitration applications and methods.

A. Related Works

In the following, we present a literature review on Game-Theoretic modeling and evaluation of human behavior, on using Game-Theoretical methods in the pHRI field, and applications of Role Arbitration and Shared Autonomy paradigms, representing our work's main background topics.

1) Game-Theory for Modeling Human Behavior: First, we want to review how human behavior can be modeled using GT formulations and which modes have been studied to understand how they can be included in the pHRI framework. Game-theoretic modeling of humans interacting with machines has been increasingly exploited recently. Typical applications of GT models are used for humans interacting with a programmed active front steering (AFS) in the shared driving of vehicles (Non-Cooperative [42], Cooperative [43], and others [44], [45]). Such works are limited to modeling interaction and lack experimental data to confirm that GT models describe interaction with real humans. Experimental evaluations are presented in [46] and in [47]. The first work presents results on the behavior of six individuals interacting with the AFS. Compared with the standard optimal control, it is shown that their interacting behavior is better described

by the Non-Cooperative formulation. Similarly, the second shows that GT-based formulation better describes the driver's behavior than the driver's classic steering control strategy.

Studies on a human-human dyad, rather than human-machine, allow an understanding of how their behavior changes according to the interacting situations. In [48], a human-human dyad performs a shared reference tracking without the possibility of communicating. It shows that the non-cooperative model is more descriptive than a model considering the partner's action as a system disturbance. Human-human interaction is also studied in [49] and [50]. These works compare the dyad with a single individual behavior. Individual players tended towards cooperative behavior to find the solution, whereas two players tended towards non-cooperation on average. Reasonably, the cooperative solution is best if the players can communicate and trust each other. If no agreement exists because there is no communication and trust, human behavior can be modeled as non-cooperative. Note that these works put the participants in non-cooperative situations on purpose (human dyads are not allowed to communicate, and the machines the humans are interacting with are programmed in a non-cooperative way). It has been proven in [51] that humans understand each other's intentions while physically interacting to perform a task, and humans adapt to Non-Cooperative behavior if the opponent behaves this way.

2) Game-Theory for pHRI: Since GT represents a robust framework to describe interactions and can describe human interaction, applications of GT modeling to pHRI control are arising in the literature. The concept of Nash Equilibrium (NE) is exploited in [52] and similarly in [53]. The NE updates the robot cost function based on the interaction force exchanged with the human. The same differential non-cooperative game-theoretic modeling is also proposed in [54] and [55]. These works exploit policy iteration to update the robot's cost function similarly compared to the previous two works presented. An observer to estimate the opponent control law is presented in [56] for the two-player game and in [57] for the multiple agents game. These works propose a universal game-theoretical framework that addresses various game-theoretical behaviors under specific control parameter tuning care. Extension to these works is in [58], where the trajectory tracking problem is addressed in the non-cooperative scenario. Finally, the authors also investigated the cooperative scenario in [59], where the weighting factor is variable to allow the adaptive impedance behavior of the robot.

3) Shared Autonomy and Role Arbitration: Finally, we want to present the most common and recent advancements in the RA and SA fields to give a background to the proposed work. The most common way to describe Shared Autonomy (SA) and Shared Control (SC) is a linear combination of human and robot control inputs as $h(u_h, u_r) = \alpha\, u_h + (1 - \alpha)\, u_r$. In [26], Shared Autonomy and Shared Control in pHRI are reviewed, highlighting the differences, pros, and cons. Ultimately, SC is more specific to the application domain and task. At the same time, SA approaches provide a favorable autonomy level adaptation feature that leverages inference of human intentions. In [60], authors investigate the objective and subjective effects of dynamic role allocation for a physical robotic assistant for a cooperative load transport task. Two dynamic Arbitration laws are proposed for effort sharing. A continuous first-order dynamical system governs one with the arbitration parameter bounded within the interval $[-1,1]$, and the other is discrete. Results show that the dynamic role allocation is objectively better than its fixed counterpart. Reference [61] proposes variable impedance control along with an assistive controller that gradually decreases to zero when the human user applies forces to pull the robot away from the predicted goal. In [62], to help a human, a strategy based on a multi-modal intent inference of human intention is developed. By looking at the natural eye-hand cooperation during a natural human manipulation, it is possible to understand the human intention of motion. The environment and the estimation introduce uncertainties, so a confidence index on the identification is defined. The arbitration weight of the robotic agent is defined as a combination of confidence in the intent inference and robotic autonomy. Role arbitration is presented in [52] and [55] as a Variable Impedance Control, where human intentions are detected from interaction force. In [63], the robot assumes two roles, with a control scheme that switches between a teaching phase (the robot is a passive follower) and an active phase (the robot is in adaptive admittance control). In [64], a controller capable of learning human behavior and providing assistive or resistive force is proposed, but no dynamic role allocation is proposed. Similarly, [65] propose a switching controller based on assistive adaptive impedance control. The stiffness parameter goes from high values to zero. This allows trajectory tracking and autonomous task execution in the first case and manual guidance in the second. In [66], a fuzzy controller introduces a cooperative coefficient according to different driving intentions, safety, and performance parameters in a cooperative driving scenario. In [67], the shared autonomy problem for the human-robot collaboration is introduced into a Partially Observable Markov Decision Problem. In [68], the Cooperative problem is addressed for the human-driver assistant problem. Finally, [69] propose a GT formulation of the problem, allowing switching between the Cooperative and the Non-Cooperative interaction models for collision avoidance in a shared human-robot driving scenario. Despite the exciting problem formulation and arbitration solution, only simulation results are presented.

4) Limitations and Problems: Based on the presented review, the following limitations are highlighted:

1) in pHRI, no comprehensive Cooperative Game-Theoretic implementation is presented in the literature;
2) Role Arbitration typically relies on Variable Impedance Control, which makes its modifications risky and complex;
3) switch between GT models (cooperative and non-cooperative) for RA is presented only in a simulated scenario and not related to the pHRI field.

B. Motivation and Contribution

Motivated that humans and robots should cooperate and take advantage of cooperation, the presented work aims to realize

This article has been accepted for inclusion in a future issue of this journal. Content is final as presented, with the exception of pagination.

4   IEEE TRANSACTIONS ON AUTOMATION SCIENCE AND ENGINEERING

a control framework for natural and mutual collaboration. Given that impedance control is standard when designing pHRI controllers, this work adopts it as low-level control to modify the robot's end-effector pose according to the interaction. According to the literature, many works aim to modify impedance control parameters online for different purposes. Adapting the impedance parameters allowing SA and RA online is generally possible, but this can be a complex and sometimes risky procedure [36]. Therefore, this work proposes considering the low-level Impedance Control as a given system on which the human and the robot can directly interact by applying forces. In this way, it is possible to consider the human and the robot as two players acting on the same system, and a Game-Theoretical formulation of the problem is allowed. The GT framework is well-suited to describe and manage conflicting objectives between rational players acting on the same system, as the literature review proposed proves.

The main contribution presented in this work is defining a Role Arbitration framework based on differential game theory to allow pHRI. Many reviewed works deal with simulated cases only, where the human is considered a rational game-theoretic player. This work focuses on the real-world application in the pHRI context, dealing with real situations and experiments to show the utility of the proposed approach. Game-theoretic approaches have already been applied in pHRI. Still, they are typically limited to the Non-Cooperative case. At the same time, this work also supports the Cooperative case in situations where the human is leading and a switching mechanism between the two models. This allows better assistance compared to the non-cooperative case.

Compared to the previous work of some of the authors [59], this work uses the knowledge of the human's desired trajectory to solve the optimal control problem. Moreover, a more complex and comprehensive role-arbitration function is defined. Finally, more experiments are evaluated to show this approach's utility in different situations.

This work aims to present a methodology that allows smooth and safe pHRI for applications requiring the co-transportation of heavy objects. Typically, there is the requirement of precise final positioning (*e.g.,* for assembly, fiber alignment in composite material draping), while the trajectory to approach that final target pose may be changed for many reasons (obstacles, ergonomics, preference, etc.).

C. Organization

The paper follows the following structure. Section I introduces the problem, presents a literature review of the main topics investigated by the proposed work, and identifies the main contribution concerning the state of the art. Section II presents the method used to manage Role Arbitration. It first derives the lower loop Impedance Control. Then, assuming the Impedance control as a given system, it formulates the Game-Theoretical problems and solutions. It defines the Role Arbitration law based on fuzzy logic, and finally, it discusses safety issues and how they can be handled with the proposed method. Section III presents the experiments and the performance evaluation criteria for comparing the proposed method with two standard pHRI controllers. Section IV presents

experimental results. Finally, Section V draws conclusions and possible future works.

1) General Notations: The most relevant Acronyms and Symbols used throughout the article are listed below

GT	Game-Theory, defines the Game-Theoretical framework
RA	Role Arbitration, defines the law that assigns the role of the leader or follower to the robot
IMP	the Impedance Control used for comparison
MG	the Manual Guidance control used for comparison
NE	the Nash Equilibrium, solution of the Non-Cooperative Game
J_i	defines a generic cost function. In the paper, different cost functions are defined and detailed
$Q_{i,j}$	defines the generic matrix that weights the state
$R_{i,j}$	defines the generic matrix that weights the control input
z	defines the state of the Mass-Spring-Damper system, composed by Cartesian positions and velocities
α	the RA parameter. In the Cooperative case, α also represents the solution to the Bargaining problem. In the Non-Cooperative case, it adjusts the value of the matrices that weigh the state.

II. METHOD

This section presents a system modeled as a virtual Cartesian Impedance subject to two external forces provided by the human and the robot, respectively. The virtual impedance produces the robot's end-effector motion in response to the measured human wrench and an additional virtual robot wrench, computed according to the GT models. Two GT models are presented, the non-cooperative and the cooperative, respectively, and the solutions of such games are provided. Finally, an arbitration function based on fuzzy logic is proposed.

A. System Modeling

Denoting with $q(t)$ the vector of joints coordinates, the standard manipulator dynamics in the joint space is given by

$$M(q)\ddot{q} + C(q,\dot{q})\dot{q} + G(q) = \tau \tag{1}$$

where $M(q) \in \mathbb{R}^{n \times n}$ is the inertia matrix, $C(q,\dot{q}) \in \mathbb{R}^{n \times n}$ is the Coriolis and centrifugal force, $G(q) \in \mathbb{R}^n$ is the gravitational force, $\tau \in \mathbb{R}^n$ is the torque control input, and $J_a(q) \in \mathbb{R}^{n \times n}$ is the Jacobian matrix. The forward kinematics gives the end-effector Cartesian pose,

$$x(t) = f(q(t))$$

where $x(t)$ denotes the Cartesian position vector and f a function that maps joint coordinates into Cartesian pose at the end-effector, and the Cartesian velocity and accelerations are given by differentiating it as

$$\dot{x}(t) = J q(t)$$

It is then possible to rewrite (1) in the Cartesian space as

$$M_x(q)\ddot{x} + C_x(q,\dot{q})\dot{x} + G_x(q) = J_a(q)^{-T} \tau \tag{2}$$

The feedback linearization is realized by imposing the control input τ as

$$\tau = J_a(q)^T [M_x(q)\ddot{x}_{ref} + C_x(q,\dot{q})\dot{x} + G_x(q)] \quad (3)$$

leading to $\ddot{x} = \ddot{x}_{ref}$, with $\ddot{x}_{ref}$ defines the desired acceleration.

Cartesian Impedance control can be implemented to make the robot's behavior responsive and compliant with human interaction. It represents a virtual mass-spring-damper system, and the human and the robot can impose forces (measured the first, virtual the latter) to move it. The impedance model in the Cartesian space is described as follows:

$$M_i(\ddot{x} - \ddot{x}_0) + C_i(\dot{x} - \dot{x}_0) + K_i(x - x_0) = u_h(t) + u_r(t) \quad (4)$$

where M_i, C_i and $K_i \in \mathbb{R}^{6\times6}$ are the desired inertia, damping, and stiffness matrices, respectively, $\ddot{x}(t)$, $\dot{x}(t)$ and $x(t) \in \mathbb{R}^6$ are the Cartesian accelerations, velocities and positions at the end-effector, x_0 is the equilibrium position of the virtual spring, and $u_h(t) \in \mathbb{R}^6$ and $u_r(t) \in \mathbb{R}^6$ represent the human (measured) and robot (virtual) effort applied to the system. The Cartesian coordinates in x are defined according to [70], with the vector $x = [p^T \; \theta^T]^T$ where p^T are the position coordinates and θ^T the set of Euler angles. This choice assumes that the angular rotation maintains limited values in the target applications.

The equation (4) can be rewritten in a linearized state-space formulation around the working point as

$$\dot{z} = Az + B_h u_h + B_r u_r \quad (5)$$

where $z = [x \; \dot{x}]^T \in \mathbb{R}^{12}$ is the state space vector, $A = \begin{bmatrix} 0^{6\times6} & J_a \\ -M_i^{-1}K_i & -M_i^{-1}C_i \end{bmatrix}$, $B_h^{12\times6} = B_r^{12\times6} = \begin{bmatrix} 0^{6\times6} \\ M_i^{-1} \end{bmatrix}$, with $0^{6\times6}$ denoting a 6×6 zero matrix and J_a the analytical Jacobian matrix, with the dimensions of the considered Cartesian components. Kinematic inversion is computed at the velocity level as

$$\dot{q}_{ref}(t) = J(q)^+ \dot{x}(t) \quad (6)$$

where $\dot{q}_{ref}(t) \in \mathbb{R}^n$, where n represents the number of joints, are the reference velocities in the joint space, $J(q)^+$ is the pseudoinverse of the analytical Jacobian matrix. Joint positions are then computed via a simple integration. Assume $\dot{q} \simeq \dot{q}_{ref}$, considering that today's robots have excellent tracking performance in the frequency range excitable by the operator.

The low-level Impedance Control loop described in (4) can be seen at a higher level as a given system, with two agents acting on it, the human and the robot, namely. A schema of the Impedance Control, assumed to be a system with two players acting on it, is visible in figure 2.

B. Differential Game Theoretic Modeling

Given the system dynamics (5), defining the players' objective is now essential. Usually, agents' objectives are formulated as cost functions that must be minimized. The objectives can be modeled as functions containing just quadratic terms. There are two main reasons for such a formulation. First, these differential games are analytically and numerically solvable. Second, this linear quadratic problem setting appears if the agents' objective is to minimize the effect of a perturbation of their nonlinear optimally controlled environment.
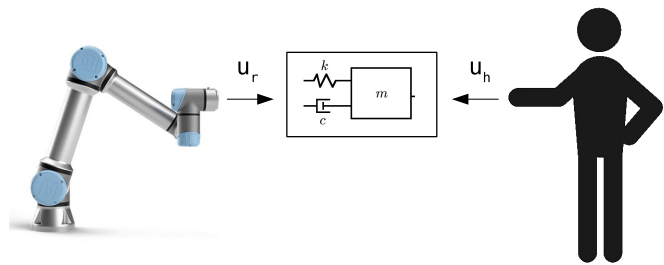

Fig. 2. The schema of the impedance system with the two external contributions.

Depending on the problem description, three main types of games are proposed. In the case players do not make any agreement and seek the optimization of their own cost without trusting each other for cooperation, we are in a Non-Cooperative situation. Conversely, in the Cooperative case, players agree to cooperate because cooperation can improve the outcome for all players to non cooperate. This situation requires trust and agreement from the opponents. The third situation describes the leader-follower case, where the followers minimize their cost function, and the leader minimizes their own based on the follower's choice. The so-called Stackelberg solutions represent its solutions. This work analyzes only the first two models, Non-Cooperative and Cooperative, because they allow easier Role Arbitration and switch from one mode to another due to intrinsic peer interaction. At the same time, the leader-follower situation requires subsequent choices. Moreover, one player always has to anticipate the action of the other, making the actual implementation challenging.

A final consideration of the human and robot objectives should be done. In general, one wants to follow a trajectory during the motion from a pose to a target one. In this paper, we define as $z_{ref,h}$ and $z_{ref,r}$ the desired trajectories that the human and the robot would follow if they were the only agent acting on the system (4). In particular, standard motion planners can compute the robot trajectory, while the human trajectory must be identified (see Sec. II-C). The objective of the two presented GT models is, in the end, to let the system in (4) evolve according to a trajectory that is obtained by a combination of the two desired trajectories.

1) Differential Non-Cooperative Game Theoretic Interaction: The non-cooperative formulation of the problem involves competition between players. The objective for each player is the minimization of their cost function. The non-cooperative aspect implies that the players are assumed not to collaborate to attain this goal. In the following, we formulate the non-cooperative problem as a two-player, non-zero-sum game. A complete treatment of non-cooperative game theory is in [71].

In the non-cooperative case, the human and the robot aim to minimize their cost functions, subject to the other influence which are given by

$$J_{h,nc} = \int_0^\infty \left[(z - z_{ref,h})^T Q_h (z - z_{ref,h}) + u_h^T R_h u_h + u_r^T R_{h,r} u_r \right] dt \quad (7)$$

and

$$J_{r,nc} = \int_0^\infty \left[(z - z_{ref,r})^T Q_r (z - z_{ref,r}) \right.$$
$$\left. + u_r^T R_r u_r + u_h^T R_{r,h} u_h \right] dt \qquad (8)$$

where $z_{ref,h}$ and $z_{ref,r}$ are the human and robot reference targets, Q_h and $Q_r \in \mathbb{R}^{12\times12}$ are weight matrices on the state, R_h and $R_r \in \mathbb{R}^{6\times6}$ are weight matrices on the player's control input and $R_{h,r}$ and $R_{r,h} \in \mathbb{R}^{6\times6}$ are weight matrices on the opponents' control input.

The non-cooperative differential game problem can be summarized as

$$\min_{u_h} \quad J_h(z, u_h, u_r)$$
$$\min_{u_r} \quad J_r(z, u_h, u_r)$$
$$s.t. \quad \dot{z} = Az + B_h u_h + B_r u_r$$
$$z(t_0) = z_0 \qquad (9)$$

Definition 1: The so-called Nash equilibrium is the set of solutions to (9). A Nash equilibrium is a situation where no player has convenience in changing its control action, formally defined as

$$J_h(z, u_h^*, u_r^*) \leq J_h(z, u_h^*, u_r)$$
$$J_r(z, u_h^*, u_r^*) \leq J_r(z, u_h, u_r^*) \qquad (10)$$

and the control actions u_h and u_r are the Nash equilibrium policies.

Two types of solutions exist based on the information players have on the current state of the system: open-loop and feedback. We consider only the feedback solutions in this work since position and force measurements are available online. In the case of linear systems as (5) and quadratic cost functions as (7) and (8), the control policies of the players are computed as

$$u_h = -K_{h,nc}(z - z_{ref,h}) \qquad (11)$$

and

$$u_r = -K_{r,nc}(z - z_{ref,r}) \qquad (12)$$

The matrices $K_{h,nc}$ and $K_{r,nc}$ are the full-state feedback matrices, computed as $K_{h,nc} = R_h^{-1} B_h^T P_h$ and $K_{r,nc} = R_r^{-1} B_r^T P_r$, where P_h and P_r are solutions of coupled Riccati equations. For simplicity, define with $S_i = B_i R_{i,i}^{-1} B_i^T$ and $S_{i,j} = B_i R_{i,i}^{-1} R_{j,i} R_{i,i}^{-1} B_i^T$, with $i = \{h, r\}$. The two coupled Riccati equations are

$$0 = (A - S_j P_j)^T P_i + P_i (A - S_j P_j)^T$$
$$- P_i S_i P_i + P_j S_{j,i} P_j + Q_i \qquad (13)$$

which can be solved as in [41]. The block diagram of the non-cooperative game interaction is in figure 3.

2) Differential Cooperative Game Theoretic Interaction: The Cooperative formulation of the problem allows agreement between the players to define a shared objective and work together toward it. The objective of each player is shared with the others, and a final, common objective is defined according to the agreement found. Players trust each other, and cooperating can improve their outcomes without hurting
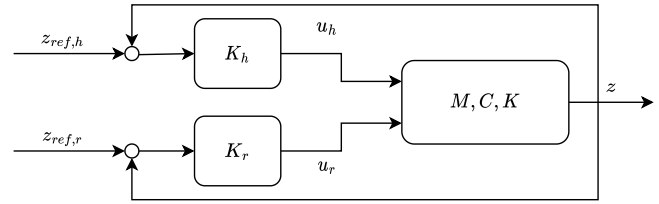

Fig. 3. The block diagram of the non-cooperative model. The $K_{h,nc}$ and $K_{r,nc}$ are obtained by the minimization of (9).

others. Each player is generally confronted with a whole set of possible outcomes from which somehow one outcome (which generally does not coincide with a player's overall lowest cost) is cooperatively selected. In the following, we present the Cooperative formulation of the two-player game, based on [40] and [72], with an extension to the agreement of a shared reference.

In a cooperative framework, the human and the robot can be seen as two agents, each one to minimize a quadratic cost function, defined as

$$J_{h,c} = \int_0^\infty \left[(z - z_{ref,h})^T Q_{h,h}(z - z_{ref,h}) \right.$$
$$\left. + (z - z_{ref,r})^T Q_{h,r}(z - z_{ref,r}) + u_h^T R_h u_h \right] dt \quad (14)$$

and

$$J_{r,c} = \int_0^\infty \left[(z - z_{ref,h})^T Q_{r,h}(z - z_{ref,h}) \right.$$
$$\left. + (z - z_{ref,r})^T Q_{r,r}(z - z_{ref,r}) + u_r^T R_r u_r \right] dt \quad (15)$$

where $J_{h,c}$ and $J_{r,c}$ are the cost that the human and the robot incur, $Q_{h,h}, Q_{h,r} \in \mathbb{R}^{12\times12}$ and $Q_{r,h}, Q_{r,r} \in \mathbb{R}^{12\times12}$ matrices that weight the state and references and $R_h, R_r \in \mathbb{R}^{6\times6}$ weights on the control input.

By cooperating, a shared objective is defined as

$$J_c = \alpha J_h + (1 - \alpha) J_r = \int_0^\infty \left(\tilde{z}^T Q_c \tilde{z} + u^T R_c u \right) dt \quad (16)$$

with $\tilde{z} = z - z_{ref}$, where z_{ref}, Q_c and R_c must be defined, and $\alpha \in (0, 1)$ represents the weight each player's cost has in the overall cost. Combining (14) and (15) into (16), after some calculations, can be obtained

$$Q_c = \alpha (Q_{h,h} + Q_{h,r}) + (1 - \alpha)(Q_{r,h} + Q_{r,r}) \qquad (17)$$

and

$$R_c = \begin{bmatrix} \alpha \hat{R}_h & 0^{6\times6} \\ 0^{6\times6} & (1-\alpha) R_r \end{bmatrix} \qquad (18)$$

Finally, defining

$$Q_h = \alpha Q_{h,h} + (1 - \alpha) Q_{h,r} \qquad (19)$$

and

$$Q_r = \alpha Q_{r,h} + (1 - \alpha) Q_{r,r} \qquad (20)$$

the reference z_{ref} is a weighted composition of the human and robot references that can be expressed as

$$z_{ref} = Q_c^{-1}(z_{ref,h} Q_h + z_{ref,r} Q_r) \qquad (21)$$

With a further step, the system in (5) becomes

$$\dot{z} = Az + Bu \qquad (22)$$

This article has been accepted for inclusion in a future issue of this journal. Content is final as presented, with the exception of pagination.

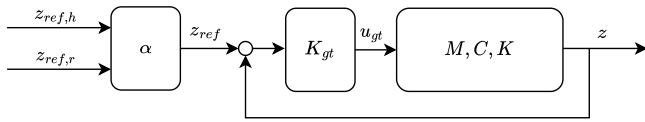FRANCESCHI et al.: HUMAN–ROBOT ROLE ARBITRATION VIA DIFFERENTIAL GAME THEORY 7

Fig. 4. The block diagram of the cooperative model. The K is obtained by the minimization of (23).

with $A \in \mathbb{R}^{12 \times 12}$ defined as before, $B \in \mathbb{R}^{12 \times 12} = [B_h \ B_r]$ and $u = [u_h \ u_r]^T \in \mathbb{R}^{12 \times 1}$.

The Linear Quadratic Differential Game problem can be finally formulated as a classical LQR problem:

$$\min_u \quad J_c = \int_0^\infty \left(z^T \, Q_c \, z + u^T \, R_c \, u \right) dt$$
$$s.t. \quad \dot{z} = A z + B u$$
$$z(t_0) = z_0 \tag{23}$$

The problem in (23) has infinite solutions lying on the Pareto frontier, depending on the parameter α.

Definition 2: A set of strategies $\mathscr{U}^* = \{u_h^*, u_r^*\}$ is called Pareto efficient if there not exists another set $\mathscr{U} = \{u_h, u_r\}$ such that

$$J_h(\mathscr{U}) \leq J_h(\mathscr{U}^*)$$
$$J_r(\mathscr{U}) \leq J_r(\mathscr{U}^*) \tag{24}$$

with at least one strict inequality.
All the solutions of problem (23) are Pareto efficient, and the choice of one or another opens a new problem, addressed in II-D. In an LQ-CGT framework, the control action u is defined as full-state feedback as

$$u = -K_{gt} \, \tilde{z} = -K_{gt} \, z + K_{gt} \, z_{ref} \tag{25}$$

with $K_{gt} = R_c^{-1} B^T P$ and matrix P solution of the Algebraic Riccati Equation (ARE)

$$0 = A^T P + P A^T - P B R_c^{-1} B^T P + Q_c$$

Note that $u = [u_h, u_r]^T$. Therefore, the human and robot control inputs can be extracted by slicing the vector of control inputs. The block diagram of the cooperative interaction model is visible in figure 4.

C. Human Reference Trajectory Estimation

The definition of a method for detecting and predicting the desired human trajectory is out of the scope of this work. Moreover, many accurate techniques exist in the literature, as proposed in [73], [74], [75], and [76], so the choice of the best human trajectory identification techniques is left to the reader. Despite this, since it is a piece of essential information to apply the control scheme proposed, it is necessary to identify a method for the prediction. In the proposed approach, we decided to implement an easy yet powerful method based on the direction of the force interaction. The human reference state is composed of position and velocity vectors as $z_{ref,h} = [x_{ref,h}^T \ \dot{x}_{ref,h}^T]^T$. The velocity component has always had a minor and typically negligible influence on human behavior, as they are proven to care only about the position and visual feedback [77], [78], [79]. Therefore, it can be set to zero

without any loss of generality, as $\dot{x}_{ref,h} = 0^{6 \times 1}$. This is a typical choice made by various works addressing human-machine interaction [44], [46], [48]. On the contrary, the pose is updated at each cycle by the following:

$$x_{ref,h}^+ = x_{ref,h}^- + K_{p,h} \, u_h \tag{26}$$

with $(^+)$ and $(^-)$ referring to the updated and previous poses, respectively, and $K_{p,h}$ defines a coefficient proportional to the human exerted force.

D. Role Arbitration Law

As already said, the solution of (23) strictly depends on the choice of α. In the Cooperative Differential Game Theory, the *Bargaining Problem* refers to the problem of choosing the best appropriate α, and different solutions are available in the literature (Nash bargaining solution [80], Kalai-Smorodinsky [81], egalitarian [82]). These methods aim to identify the best compromise between players so that everyone has the incentive to cooperate rather than compete against each other. The solution found is static, and the game proceeds by minimizing (23).

In the proposed control schema, the value of α is changed dynamically on the fly according to some defined law, allowing the Role arbitration between the human and the robot. Indeed, this work aims to make the robot assistive, capable of following human intentions, assisting humans, and taking control over humans to avoid undesired situations.

Four main undesired situations are identified:

a) singularities
b) proximity to objects
c) proximity to workspace limits
d) distance to the reference target position

Remark 1: Proximity to joint limits is not directly considered, as in the computation of the manipulability index, it is already included, as described below.

To avoid configurations close to singularities, the manipulability index μ is taken into account, defined as in [83]:

$$\mu = P\sqrt{det(\mathbf{J}(\mathbf{q})\mathbf{J}(\mathbf{q})^T)}, \tag{27}$$

with penalty factor P, similar to the one introduced in [84] used to scale the manipulability to account for joint limits. P are computed separately for each joint j, as

$$P_j = 1 - e^{-k\frac{(q_j - q_j^{lb})(q_j^{ub} - q_j)}{(q_j^{ub} - q_j^{lb})^2}}, \tag{28}$$

where k is a scaling factor that can be used to adjust the behavior near joint limits, q_j is the current position of the joint j, and q_j^{ub} and q_j^{lb} are the upper and lower bounds, respectively.

The proximity to objects d_o is measured as the minimum distance between any robot link and any object in the environment, possibly excluding objects that must be manipulated.

$$d_o = \min(robot - objects) \tag{29}$$

The proximity to workspace limits d_{ws} represents the Euclidean distance between the current Cartesian position of

This article has been accepted for inclusion in a future issue of this journal. Content is final as presented, with the exception of pagination.

8

IEEE TRANSACTIONS ON AUTOMATION SCIENCE AND ENGINEERING

(a) manipulability membership function

(b) distance to collisions membership function

(c) distance to workspace boundaries membership function

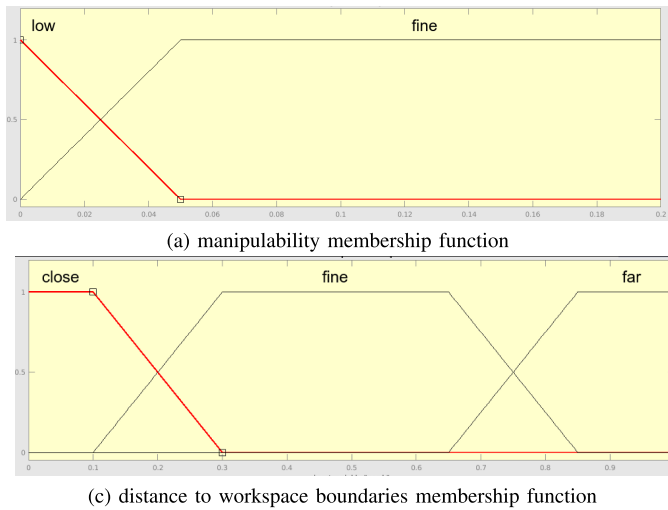(d) distance to target pose membership function

Fig. 5.   Input membership functions to the Fuzzy Logic System.

the robot TCP and the boundaries specified according to the application.

$$d_{ws} = \|x^{ee} - x^{ws}\| \tag{30}$$

with x^{ee} and x^{ws} denoting the Cartesian positions of the end-effector and the workspace boundaries, respectively.

The distance to the reference target position d_{trg} is measured as the Euclidean distance between the current end-effector position and the target pose of the task (*e.g.,* pick/place pose).

$$d_{trg} = \|x^{ee} - x^{trg}\| \tag{31}$$

with x^{trg} denoting the target position of the end-effector.

These four indices allow defining the proper α, allowing for Role Arbitration. It is defined as a Fuzzy Logic System (FL) that accepts as inputs the four indices and returns the value of α. In figure 5, the four membership functions related to the four indices are visible. The following rules are defined:

$$
\begin{cases}
\text{if } (\mu \text{ is } low) \text{ or } (d_o \text{ is } low) \text{ or } (d_{ws} \text{ is } close) \\
\qquad \text{or } (d_{trg} \text{ is } close) \text{ then } \alpha \text{ is } low \\[6pt]
\text{if } (\mu \text{ is } low) \text{ or } (d_o \text{ is } low) \text{ or } (d_{ws} \text{ is } far) \\
\qquad \text{or } (d_{trg} \text{ is } close) \text{ then } \alpha \text{ is } low \\[6pt]
\text{if } (\mu \text{ is } fine) \text{ or } (d_o \text{ is } ok) \text{ or } (d_{ws} \text{ is } fine) \\
\qquad \text{or } (d_{trg} \text{ is } far) \text{ then } \alpha \text{ is } high \\[6pt]
\text{if } (\mu \text{ is } fine) \text{ or } (d_o \text{ is } ok) \text{ or } (d_{ws} \text{ is } fine) \\
\qquad \text{or } (d_{trg} \text{ is } medium) \text{ then } \alpha \text{ is } shared
\end{cases}
\tag{32}
$$

Processing the four membership functions through the above rules allows defining the proper α, with its membership function visible in figure 6. Identifying a threshold value of $\alpha = \alpha_{th}$ makes switching from the Cooperative to the non-cooperative case possible, allowing Role Arbitration. When α is high, the cooperative interaction model is selected, and the human can
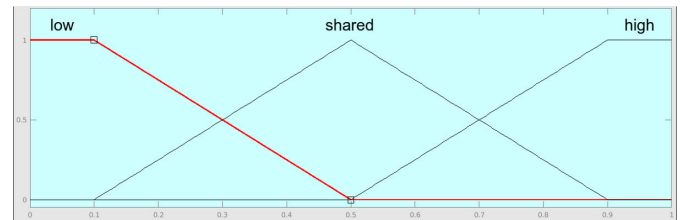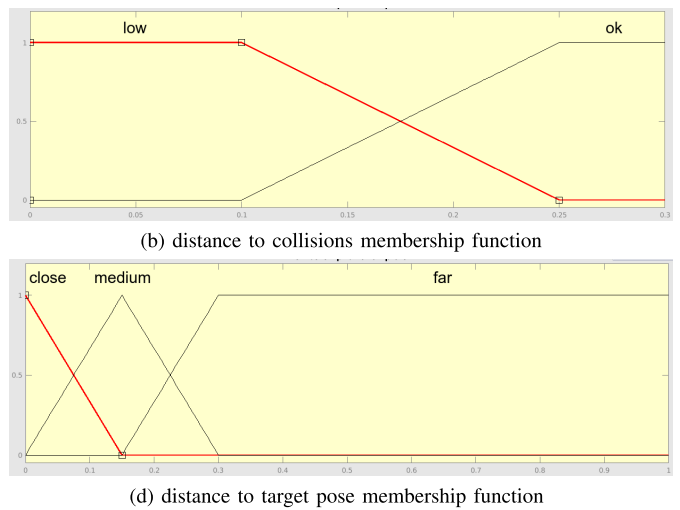
Fig. 6.   Output membership function of the FLS that defines α.
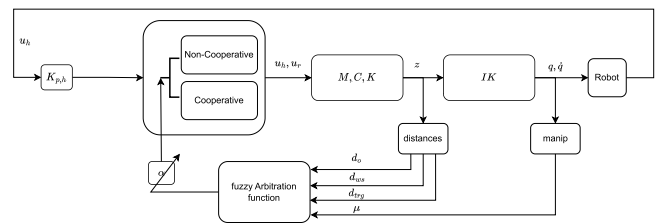
Fig. 7.   The block diagram of the arbitration mechanism. The variable α allows switching between cooperative and non-cooperative models.

fully control the task and move the robot freely, enhanced by the robot assistance u_r. Conversely, when α is low, the non-cooperative interaction model is selected, and the robot takes control over the human by applying a virtual force u_r to recover the original safe trajectory. The block diagram of the arbitration control is in figure 7.

Remark 2: By varying the parameter α, also the matrices Q_h, Q_r, R_h and R_r vary. In the Cooperative case, how they vary is straightforward, and it is described by (17) and (18). In this case, the parameter α also represents the solution to the Bargaining problem. In the Non-Cooperative case, the matrices are computed as (19) and (20). The value of the matrices R_h and R_r are kept constant.

E. Safety Considerations

The method proposed does not directly address the safety issues that arise when pHRI is considered. Therefore, some considerations are given. According to the standard rules defined by the ISO in [85], [86], and [87], safety depends

This article has been accepted for inclusion in a future issue of this journal. Content is final as presented, with the exception of pagination.

FRANCESCHI et al.: HUMAN–ROBOT ROLE ARBITRATION VIA DIFFERENTIAL GAME THEORY
9

on and is evaluated considering the entire application and not the single modules such as the robotic platform, its control, and the other modules alone.

According to the standards, the robot at the end-effector should not move faster than 250 mm/s to certify the application. It should also stop if the external forces and power exceed a threshold according to the so-called Power Force Limitation (PFL).

Despite being hard to make sure that the application is safe according to the standards, the proposed FL arbitration law can handle such limitations within certain limits. Indeed, by defining some additional rules, the FL arbitration can prevent the robot from moving too fast or colliding unsafely with the human. By preventing such events, robot safety stops triggered by modules and sensors certified according to the standards can be reduced.

For example, the proposed fuzzy logic arbitration can handle the speed limitation. Indeed, the nominal trajectory is computed to comply with the limited speed constraint. The FL can include monitoring the speed, and the role of the leader can be assigned to the robot as close as the end-effector speed approaches the limit if the human tries to move faster.

PFL requires that, in the case of a collision with a human, the power and force are granted to be below a certain threshold. Such a threshold depends on the type of collision (free body or pinch) and the body area where it might happen. To avoid direct collisions with the human body, a camera system can track the human body position, the human body can be modeled as an environmental obstacle, and (29) allows for taking this distance into account. Moreover, a rule that monitors the robot's position to the human body parts can also be added. For example, if it comes too close to the human head, the FL arbitration should allow the robot to lead the action far from it. It can be handled by measuring the height of the robot end-effector or directly by using a skeleton tracker if available. It is also possible to add danger zones as described in [88] and include them in the FL arbitration law. Of course, this approach should not consider the human arm that is directly in contact with the robot (if no co-manipulated object is considered). Otherwise, the distance between the human and the robot will always be obviously zero.

The presented cases do not guarantee the certification of the collaborative application, which requires the safety stops of the robot. On the contrary, they can prevent the robot from incurring such situations, allowing it also to reduce safety stops.

III. EXPERIMENTS

Three sets of experiments are designed to test the method's validity. In all scenarios, the human and the robot must reach a target position and return to the starting point. In the first case, a collision object is added to the scene, but the human does not know its presence. In the second scenario, the human knows the presence of an object, while the robot doesn't. The third case does not involve collision objects but requires reaching an intermediate target point that the robot does not know. The test cases are designed to simulate these three real-world scenarios:

a) the human and the robot are co-manipulating an object, possibly significant, that may impede the human's view

of some environmental feature. The robot knows the obstacle's presence and helps the human avoid it. Another situation can happen when the obstacle is behind the human, and he does not see it;

b) a dynamical collision object is placed in the middle of the robot's trajectory, and the human sees it and drives the robot far from possible collisions;

c) a task is mainly repeatable. Still, some exceptions can sometimes require an additional operation (e.g., during object sorting, most objects must be placed in a container, but some objects must be redirected for some additional operation due to poor quality).

The proposed approach is compared with two other controller methodologies typically used to execute such tasks: standard manual guidance (MG) and a standard impedance control (IMP). The first controller (MG) represents a standard when an operator guides the robot, and it acts as a follower. Typical applications are learning-from-demonstration or robotic assistance for load reduction. The second controller (IMP) is typical in pHRI as it allows compliance and a robot that modifies its trajectory according to external forces.

Remark 3: The same control can obtain the three controller behavior by switching off the robot contribution for IMP (*i.e.,* $u_r = 0$ in (4)), switching off the robot contribution, and setting null the robot stiffness for MG (*i.e.,* $u_r = 0$, and $K_i = 0$ in (4)).

Remark 4: The trajectories are precomputed using Moveit! and then used for all the cases to make the experiments fully comparable.

A. Evaluation Criteria

The following indexes are defined and evaluated to compare the three controllers. The interaction force is evaluated as a measure of the robot's assistance to the human. The less the force is, the better the robot assists the human. The interaction force is measured as

$$\mathscr{F} = \int_{T_{start}}^{T_{end}} \frac{\|f(t)\|}{T} \, dt \tag{33}$$

it is normalized over T in which a force greater than a threshold (1N) is measured.

An index measures the percentage of points in the measured trajectory in which the robot is closer than 1mm to the obstacle to measure the obstacle avoidance capability. The index is defined as

$$\mathscr{C}^{\%} = \frac{n_c}{n_p} 100 \tag{34}$$

with n_c and n_p indicating the number of points in a collision (*i.e.* the robot is closer than 1mm to the obstacle) and the total number of points in the trajectory, respectively.

An index measures the percentage of points in the measured trajectory in which the robot's end-effector violates the safe workspace boundaries (in this work, it is set to 850mm as from the UR5 datasheet) to measure the capability in avoiding the violation of the workspace boundaries. The index is defined as

$$\mathscr{W}\mathscr{S}^{\%} = \frac{n_{ws}}{n_p} 100 \tag{35}$$

This article has been accepted for inclusion in a future issue of this journal. Content is final as presented, with the exception of pagination.

10   IEEE TRANSACTIONS ON AUTOMATION SCIENCE AND ENGINEERING
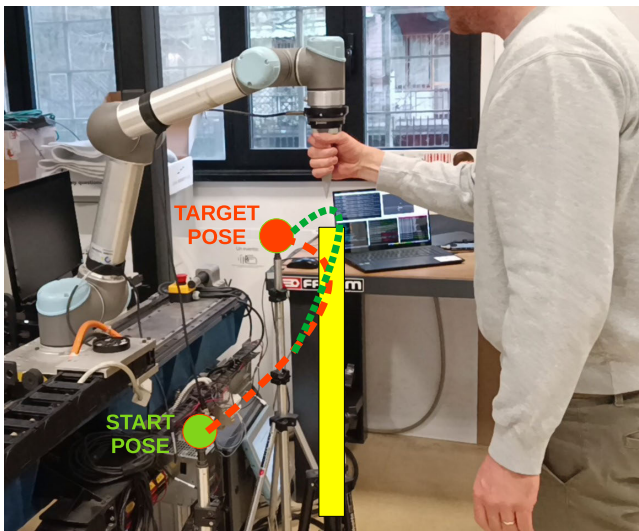

Fig. 8. Experimental setup during the execution of obstacle avoidance experiment. The human is driving the robot to avoid the physical obstacle highlighted by the yellow rectangle in the picture. The nominal robot's trajectory is in dashed red. In green is the new trajectory after the human intervention to avoid the obstacle. In the real setup, the start pose (green circle), the target pose (red circle), and the obstacle (yellow rectangle) are indicated by tripods to give the human a reference.
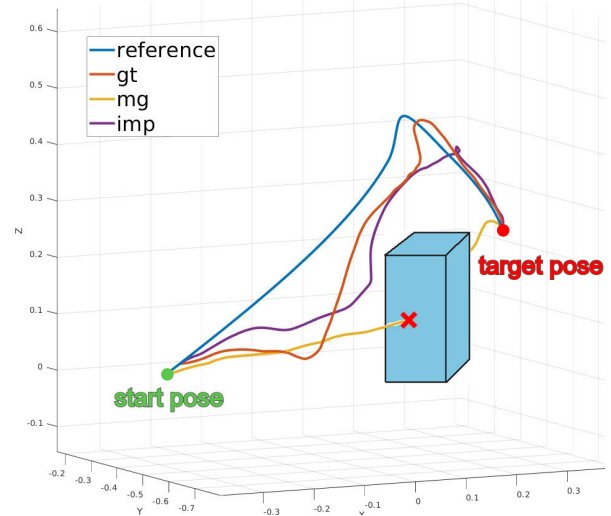

Fig. 9. The end-effector trajectories in the Cartesian space in the first set of experiments. The GT and IMP controllers can safely avoid the obstacle by imposing force on the human. The MG controller cannot impose any force, and it collides.

with n_{ws} and n_p indicating the number of points that violate workspace boundaries (*i.e.* the robot end-effector is far more than 850mm from the robot base) and the total number of points in the trajectory, respectively.

Finally, since the proposed control also allows precise robot positioning at target points (e.g., pick/place target poses), an index evaluates the capability to precisely reach a target pose, defined as (31), measured when the action is considered concluded.

$$d_{trg} = \left\| x^{ee} - x^{trg} \right\| \qquad (36)$$

This same index is used to measure the capability of reaching target points known to the robot and the additional via point in case (c), which is unknown to the robot.

B. Experimental Setup

A total of 5 participants (age 28 $\pm$ 3.5) were involved in the testing. The participants have different confidence and previous experience with using robots in general and pHRI tasks. In particular, one participant had no experience with robots at all. The participants were instructed to move the robot tip from start to target pose and were told that the robot could take control over the human in some situations. Participants were asked to let the robot lead if they sensed that the robot was taking control.

The robotic platform is a Universal Robot 5 controlled in joint velocity at a frame rate of 125 Hz. The interaction force is measured at 100 Hz with a Robotiq FT300 sensor mounted at the robot end-effector. A handle is mounted after the sensor, allowing the human to grasp and interact with the robot. The robotic setup during the execution of experiments when the human is leading the robot to avoid an obstacle is visible in figure 8.

The parameters used are as follows. $Q_{h,h} = diag([1, 1, 1, 0.0001, 0.0001, 0.0001])$, $Q_{h,r} = 0^{6 \times 6}$ and $R_h = diag([0.0005, 0.0005, 0.0005])$ and $Rr = diag([0.0001, 0.0001, 0.0001])$.[1] The values of the impedance parameters in (4) are set to $M_i = diag([10, 10, 10])$, $D_i = diag([100, 100, 100])$ and $K_i = diag([0, 0, 0])$ for the standard manual guidance and the GT experiments, while $K_i = diag([200, 200, 200])$ for the standard impedance control. For a complete system response analysis with different parameters tuning, please refer to [89].

The values for the human are computed offline via Inverse Optimal Control as in [79]. Despite the human cost function values possibly changing according to the task, the subject, and the different stages of the task, the choice of using fixed values can be justified for several reasons. First of all, the role arbitration mechanism is the fundamental module that changes the assistance level of the robot, which strictly depends on the value of α. Both the value of α and the human cost function influence the game's outcome. Still, the value of α has a significantly higher impact with respect to the human cost function, provided that the values used to describe the human cost function are reasonable within certain tolerances (we selected an average value; indeed, such a value can possibly change, but changes are within a restricted range around the value we use). Note that it is always possible to implement online techniques to recover such parameters on the fly and for different phases of the task, as demonstrated by various works [90], [91], [92], [93]. The robot's parameters are set according to previous studies to assist when required and provide strong interaction when there is no agreement. Note

---

[1] All these values are normalized with respect to $Q_{h,h}(1,1)$. In Optimal Control problems, the minimization of J_i equals the minimization of λJ_i, with λ positive value. Therefore, since the parameters $Q_{h,h}$ and R_h come from Inverse Optimal Control studies, they can be normalized to any arbitrary value. The small values of $Q_{h,h}$ relative to the velocity components of the state indicate that humans do not care about the velocity compared with the tracking error. The small values of R_h indicate that humans prefer to minimize the tracking error rather than the effort required to track it.

This article has been accepted for inclusion in a future issue of this journal. Content is final as presented, with the exception of pagination.

FRANCESCHI et al.: HUMAN–ROBOT ROLE ARBITRATION VIA DIFFERENTIAL GAME THEORY 11

(a) Variation of α during the task
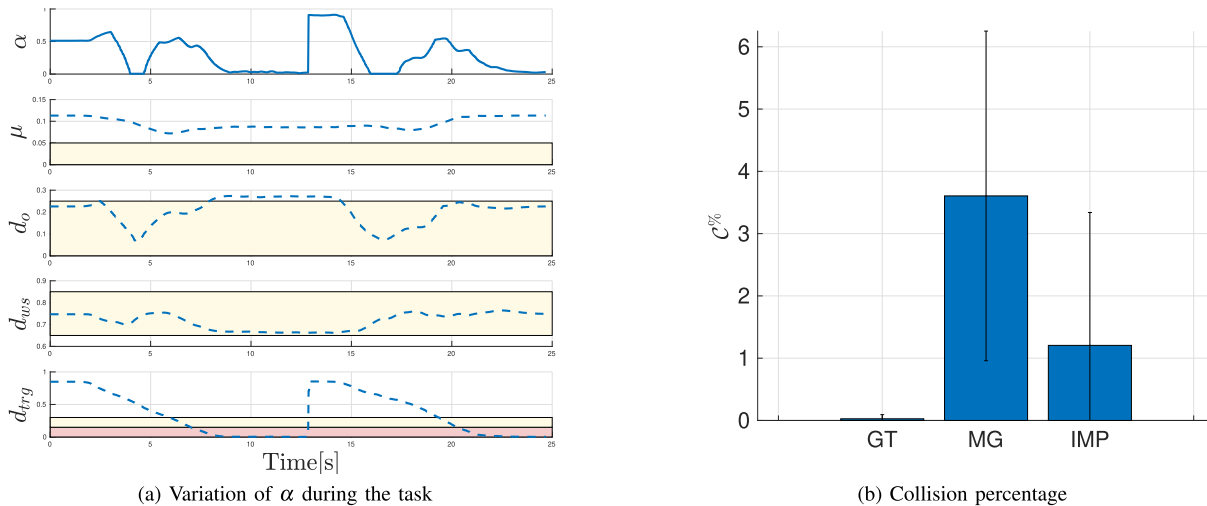
(b) Collision percentage

Fig. 10. Experiment A: in this case, the human does not know the obstacle's presence.

that this work uses the same parameters for each user. The performance and the user experience can be further improved by adding a tuning tailored to each user's preferences. For a methodology to tune the parameters according to each subject preference, please see [94]. The matrices Q_h and Q_r are defined as in the cooperative case for all the cases. This means that, in the cooperative case, Q_h and Q_r are defined as in II-B2 following (19) and (20). In the non-cooperative case, equations (7) and (8) in section II-B1 use Q_h and Q_r. To let the Role Arbitration be smooth and continuously variable, we also update values of Q_h and Q_r according to the same update used for the cooperative case, following (19) and (20).

During the experiments, the FL arbitration module is in charge of selecting the appropriate role for the human and the robot (*i.e.*, the value of α) according to the current status of the tasks. Therefore, during each experiment, the value of α varies. By defining a threshold value of α ($\alpha_{th} = 0.5$, in this work), the robot selects the cooperative or the non-cooperative behavior according to $\alpha > \alpha_{th}$ and $\alpha < \alpha_{th}$, respectively.

IV. RESULTS

This section presents the results relative to the three sets of experiments.

A. Experiment With the Object Unknown to the Human

In the first set of experiments, the robot knows the presence of an obstacle and leads the human away from an object known to the robot. The goal is to move the robot end-effector from an initial position to a target position, then, after a slight pause, move back to the initial position. In the middle of the trajectory is placed a virtual object. The robot knows the obstacle's presence and position, but the human does not. The robot's nominal trajectory is computed to be collision-free, considering the obstacle known to the robot.

Figure 10a shows the arbitration parameter α variation during the task. In particular, around second 4, the robot approaches the object, and d_o is low. Moreover, d_{ws} increases, making α low and the robot close to its nominal trajectory.
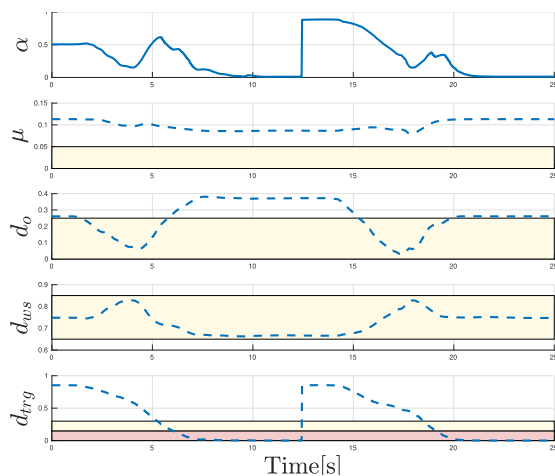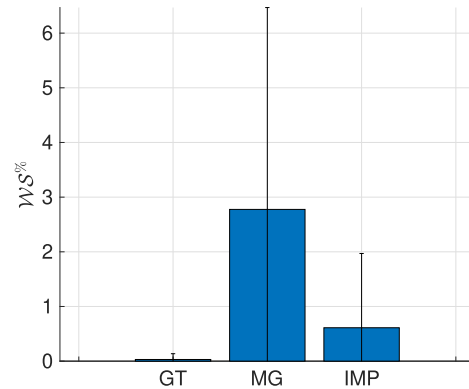
This experiment computes the capability of the three controllers to avoid any collision. Figure 10b shows an average of the index (34) computed for all the subjects. As clearly visible, in the MG case, because the robot cannot exert any force, the human is not aware of the robot's intention and collides with the virtual obstacle. In the GT and IMP cases, the human can almost always avoid the obstacle, even if it is unknown, because the robot pulls the human to its collision-free trajectory, helping him avoid it. In this case, GT and IMP behave similarly in proximity to the obstacle.

Figure 9 shows the trajectories followed by the robot tip with the three controllers and the nominal collision-free trajectory computed by the motion planner. As visible, the IMP and GT controllers allow the robot to pull the human and its tip close to the nominal collision-free trajectory, allowing the task's success. On the contrary, in the MG case, no force can be exerted, and the robot cannot prevent collision with the obstacle.

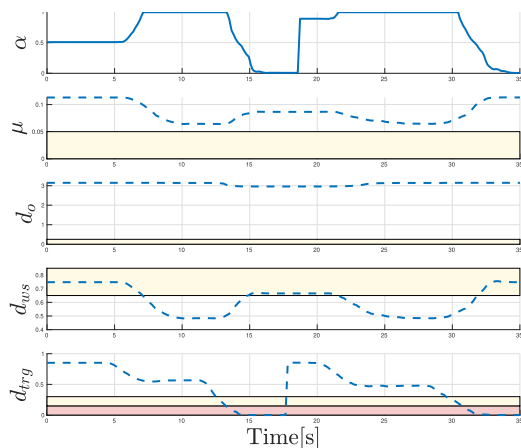### B. Experiment With the Object Unknown to the Robot

In this experiment, the human leads the robot away from an object known only to the human.

In this case, because the human knows precisely where the obstacle is, it is easier for them to avoid it. Hence, the index (34) was found to be always zero, and it is not shown here. Conversely, because the human can move the robot to avoid the obstacle, this may violate workspace boundaries. Indeed, during the test with the MG controller, two subjects exceeded workspace boundaries while avoiding the obstacle (the robot was straight), leading to swift joint motions of the elbow joint and finally to the robot's emergency stop. Figure 11b shows an average of the workspace boundaries violation for the three controllers, computed as (35) (the two occurrences described above are not used for index computation, and an additional trial was done). The GT controller is the one that better avoids workspace boundary violation, allowing safer deformations compared with the other two controllers.

This article has been accepted for inclusion in a future issue of this journal. Content is final as presented, with the exception of pagination.

12   IEEE TRANSACTIONS ON AUTOMATION SCIENCE AND ENGINEERING

(a) Variation of   during the task

(b) Workspace boundaries.

Fig. 11.   Experiment B: the human deviates from nominal trajectory to avoid an obstacle unknown to the robot.

(a) Variation of α during the task.
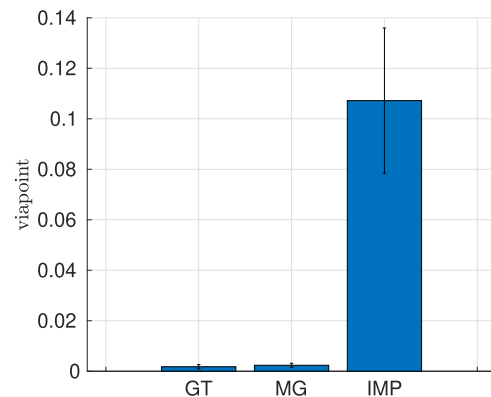
(b) Proximity to the additional via-point not known to the robot.

Fig. 12.   Experiment C: trajectory deformation.

As visible from figure 13, in the case of MG and partially in the IMP, the trajectory modified by the human exceeds the safe workspace boundaries. The workspace boundaries are, in this work, designed according to the UR specifications. This means the robot can exceed it, as happens in this experiment. Most positions can be reached but with restrictions on the tool orientation because the robot cannot reach far enough in some situations.

C. Experiment With Additional Target Point

The third case is presented here. The initial and final points of the task are the same as in the previous experiment, and the robot's nominal trajectories are the same. An additional target point is in between, and the human is asked to reach it. Therefore, instead of directly moving toward the target point, the human has to modify the robot's nominal trajectory to reach an intermediate way-point precisely. No obstacles are involved in the scene, and the robot allows trajectory deformations as long as the tip is far from the target pose.

The variation of the various indices is visible in figure 12a. As visible, the only phases where the robot leads happen near

the target pose, granting precise position reach. Instead, during the task execution, the arbitration parameter lets the human lead (with an exception at the beginning of the task because the starting position is close to the WS boundaries), allowing the robot's behavior to be comparable to the one of the MG control. The precision of reaching the intermediate way-point is measured by (36), and results of the comparison with MG and IMP are shown in 12b. The robot's behavior is comparable to the one of the MG. Therefore, the precision of reaching the target point is comparable between GT and MG, showing good performances. On the contrary, the IMP control does not allow substantial trajectory deformations nor the robot to slow down/stop at a precise way-point, leading to bad performances.

Figure 14 shows the trajectory executed with the three controllers to perform this task. As visible, the target via point is unreachable in the IMP case. This happens because the robot prevents the human from reaching it since it does not adapt to the human's intentions. Indeed, the IMP controller aims at following the predefined trajectory, allowing just minor adjustments given by the interaction, and too high forces are required to modify the trajectory substantially.

This article has been accepted for inclusion in a future issue of this journal. Content is final as presented, with the exception of pagination.

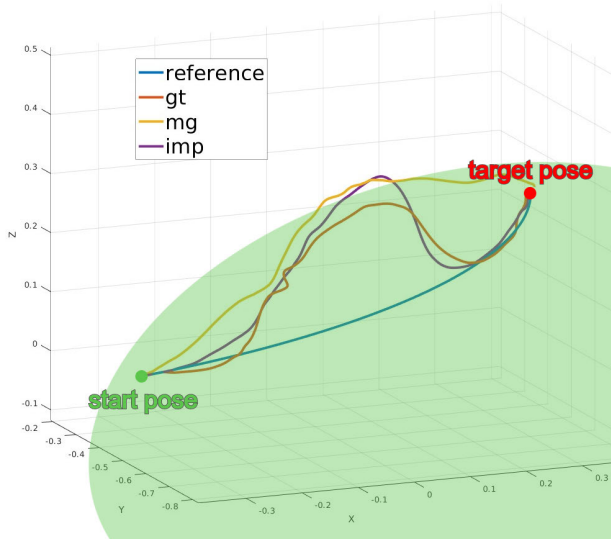FRANCESCHI et al.: HUMAN–ROBOT ROLE ARBITRATION VIA DIFFERENTIAL GAME THEORY

13

Fig. 13. The end-effector trajectories in the Cartesian space in the second set of experiments (humans must avoid an obstacle). The MG and IMP controllers slightly exceed the workspace boundaries. The RA framework keeps the GT controller below the dangerous robot's over-extension. The light green area represents the allowed workspace.
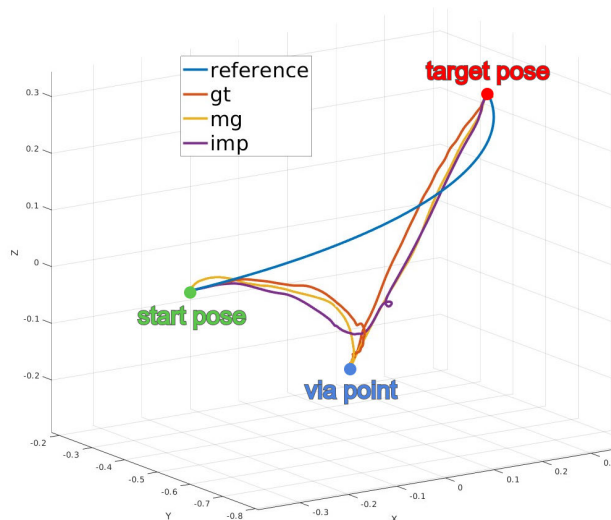

Fig. 14. The end-effector trajectories in the Cartesian space in the third set of experiments (humans must reach an additional via point). The IMP controller does not allow reaching the desired via point because it pulls the end-effector toward the nominal trajectory far from the via point. The GT and MG controllers allow for trajectory modification and reach precisely the additional via point.

D. General Considerations

In this subsection, performances comparable for the three controllers are analyzed.

Figure 15 shows results for the force index in (33). In general, the IMP controller is the one that presents a higher required force to complete the task for all the cases. This happens because the controller treats human forces as external disturbances, and the virtual spring always tends to steer the system to the reference position.

MG and GT show comparable forces in the case the human knows the obstacle and moves the robot to avoid it. Considering the case where the robot knows the obstacle's
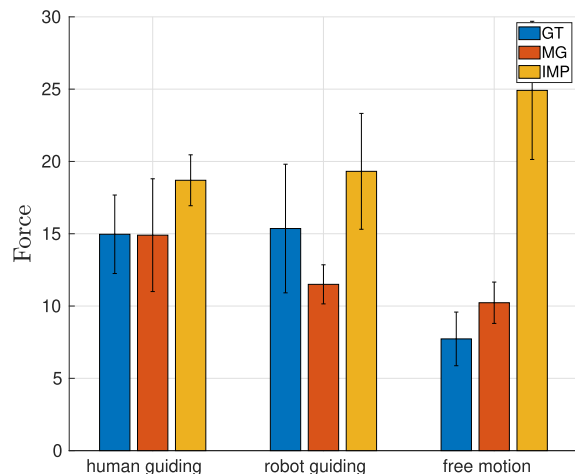

Fig. 15. Forces exerted by the human while performing the task with the three controllers. P-values are (0.9560, 0.0067, 0.0130, 0.0126, 0.0005, 0.0003). The null hypothesis is rejected between GT and MG if the human deviates from the robot. The null hypothesis is rejected between GT and IMP if the robot deviates from the human trajectory. The null hypothesis is confirmed for the free robot motion.
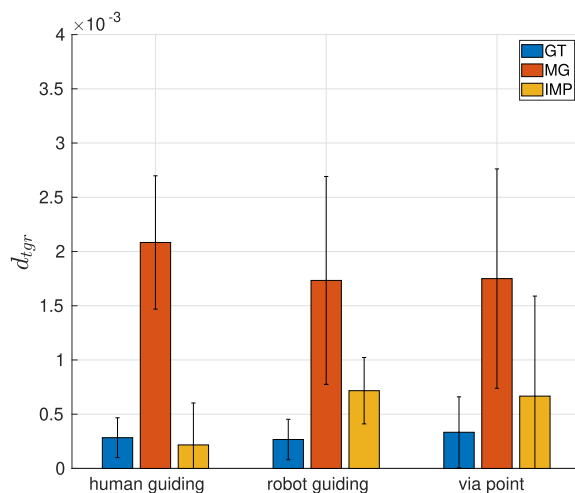

Fig. 16. Target position reaching.

presence, the GT case exchanges more force because the robot must impose a force to attract the robot end-effector on the safe collision-free nominal trajectory. Such a force represents a haptic channel of communication that makes the human aware of the robot wanting to take the lead. In the MG case, the exchanged force is lower because the robot follows the human without steering capability. This situation is not applicable because it leads the system to a collision. Finally, in the case of additional via point reaching, the MG control requires additional force if compared with the GT control because it always requires force to move in the same direction. In the GT case, the force can be reduced as the robot assists in moving in the desired direction.

The capacity to reach with precision the final point is in figure 16. As expected, in the MG case, the capacity to match the final point is left to human ability, leading to the highest values for all three experiments. The performances of GT and IMP are comparable, as the two methods are very similar in behavior when the arbitration parameter α is low.

Finally, note that the robot's nominal paths are precomputed for each experimental scenario and kept the same for each experiment. This choice is made to compare each experiment avoiding dependencies of the various indexes (in particular (33), (34) and (35)) from different path lengths. This may raise the reasonable question of how different paths and path lengths influence the index evaluations. In general, different values for the indexes are expected with varying path lengths, as they strictly depend on the interaction time or the percentage of interaction along the entire path. Despite this, similar results are expected when comparing the same controllers on the same path, even if it is shorter or longer with respect to the ones proposed in this work. For example, consider a longer path for the experiment presented in section IV-A. For sure, the values visible in 10b will be different, as the percentage computed depends on the path length. Despite this, the proposed method still allows the user to avoid the unknown obstacle better than the MG and IMP controllers.

V. Conclusion

This work proposes applying differential game theory models for the role arbitration between a human and a robot. Both Cooperative and Non-Cooperative solutions are addressed and utilized in the cases more suitable for one or the other. A Fuzzy Logic System defines an arbitration function capable of considering various dangerous situations to modify the arbitration parameter α. This arbitration function is a hybrid controller that behaves as empowering manual guidance when dangerous situations are not foreseen while moving to a behavior closer to impedance control when the robot approaches dangerous situations. Experiments show that the proposed controller outperforms the other two in various situations.

Future works will address a Model Predictive Control formulation of the problem, allowing the robot to foresee dangerous situations and anticipate the Role Arbitration as needed. A deeper understanding of the future human trajectory is needed to do this. Hence, future works will also address human trajectory prediction over a finite horizon, possibly exploiting artificial intelligence methods. The code to compute the GT control inputs is available here: github.

References

[1] E. Prati, V. Villani, F. Grandi, M. Peruzzini, and L. Sabattini, "Use of interaction design methodologies for human–robot collaboration in industrial scenarios," *IEEE Trans. Autom. Sci. Eng.*, vol. 19, no. 4, pp. 3126–3138, Oct. 2022.

[2] E. Prati, M. Peruzzini, M. Pellicciari, and R. Raffaeli, "How to include user experience in the design of human–robot interaction," *Robot. Comput.-Integr. Manuf.*, vol. 68, Apr. 2021, Art. no. 102072.

[3] R. Jahanmahin, S. Masoud, J. Rickli, and A. Djuric, "Human–robot interactions in manufacturing: A survey of human behavior modeling," *Robot. Comput.-Integr. Manuf.*, vol. 78, Dec. 2022, Art. no. 102404.

[4] S. Proia, R. Carli, G. Cavone, and M. Dotoli, "Control techniques for safe, ergonomic, and efficient human–robot collaboration in the digital industry: A survey," *IEEE Trans. Autom. Sci. Eng.*, vol. 19, no. 3, pp. 1798–1819, Jul. 2022.

[5] V. Villani, F. Pini, F. Leali, and C. Secchi, "Survey on human–robot collaboration in industrial settings: Safety, intuitive interfaces and applications," *Mechatronics*, vol. 55, pp. 248–266, Nov. 2018.

[6] A. De Santis, B. Siciliano, A. De Luca, and A. Bicchi, "An atlas of physical human–robot interaction," *Mechanism Mach. Theory*, vol. 43, no. 3, pp. 253–270, 2008.

[7] N. Hogan, "Impedance control: An approach to manipulation: Part I—Theory," *J. Dyn. Syst., Meas., Control*, vol. 107, no. 1, pp. 1–7, Mar. 1985.

[8] S. Haddadin and E. Croft, *Physical Human–Robot Interaction*. Cham, Switzerland: Springer, 2016, pp. 1835–1874.

[9] D. P. Losey and M. K. O'Malley, "Trajectory deformations from physical human–robot interaction," *IEEE Trans. Robot.*, vol. 34, no. 1, pp. 126–138, Feb. 2018.

[10] S. S. Ge, Y. Li, and H. He, "Neural-network-based human intention estimation for physical human–robot interaction," in *Proc. 8th Int. Conf. Ubiquitous Robots Ambient Intell. (URAI)*, Nov. 2011, pp. 390–395.

[11] M. Sharifi, S. Behzadipour, and G. R. Vossoughi, "Model reference adaptive impedance control in Cartesian coordinates for physical human–robot interaction," *Adv. Robot.*, vol. 28, no. 19, pp. 1277–1290, Oct. 2014, doi: 10.1080/01691864.2014.933125.

[12] L. Roveda, S. Haghshenas, M. Caimmi, N. Pedrocchi, and L. M. Tosatti, "Assisting operators in heavy industrial tasks: On the design of an optimized cooperative impedance fuzzy-controller with embedded safety rules," *Frontiers Robot. AI*, vol. 6, p. 75, Aug. 2019.

[13] L. Roveda et al., "Fuzzy impedance control for enhancing capabilities of humans in onerous tasks execution," in *Proc. 15th Int. Conf. Ubiquitous Robots (UR)*, Jun. 2018, pp. 406–411.

[14] W. He, C. Xue, X. Yu, Z. Li, and C. Yang, "Admittance-based controller design for physical human–robot interaction in the constrained task space," *IEEE Trans. Autom. Sci. Eng.*, vol. 17, no. 4, pp. 1937–1949, Oct. 2020.

[15] J. Luo, D. Huang, Y. Li, and C. Yang, "Trajectory online adaption based on human motion prediction for teleoperation," *IEEE Trans. Autom. Sci. Eng.*, vol. 19, no. 4, pp. 3184–3191, Oct. 2022.

[16] J. Dong, J. Xu, Q. Zhou, and S. Hu, "Physical human–robot interaction force control method based on adaptive variable impedance," *J. Franklin Inst.*, vol. 357, no. 12, pp. 7864–7878, Aug. 2020.

[17] F. Müller, J. Janetzky, U. Behrnd, J. Jäkel, and U. Thomas, "User force-dependent variable impedance control in human–robot interaction," in *Proc. IEEE 14th Int. Conf. Autom. Sci. Eng. (CASE)*, Aug. 2018, pp. 1328–1335.

[18] F. Ficuciello, L. Villani, and B. Siciliano, "Variable impedance control of redundant manipulators for intuitive human–robot physical interaction," *IEEE Trans. Robot.*, vol. 31, no. 4, pp. 850–863, Aug. 2015.

[19] B. Yao, Z. Zhou, L. Wang, W. Xu, Q. Liu, and A. Liu, "Sensorless and adaptive admittance control of industrial robot in physical human–robot interaction," *Robot. Comput.-Integr. Manuf.*, vol. 51, pp. 158–168, Jun. 2018.

[20] L. Roveda et al., "Human–robot cooperative interaction control for the installation of heavy and bulky components," in *Proc. IEEE Int. Conf. Syst., Man, Cybern. (SMC)*, Oct. 2018, pp. 339–344.

[21] L. Roveda et al., "Model-based reinforcement learning variable impedance control for human–robot collaboration," *J. Intell. Robotic Syst.*, vol. 100, no. 2, pp. 417–433, Nov. 2020.

[22] L. Roveda, A. Testa, A. A. Shahid, F. Braghin, and D. Piga, "Q-learning-based model predictive variable impedance control for physical human–robot collaboration," *Artif. Intell.*, vol. 312, Nov. 2022, Art. no. 103771.

[23] Y. Li and S. S. Ge, "Human–robot collaboration based on motion intention estimation," *IEEE/ASME Trans. Mechatronics*, vol. 19, no. 3, pp. 1007–1014, Jun. 2014.

[24] H.-Y. Li, I. Paranawithana, L. Yang, and U.-X. Tan, "Variable admittance control with robust adaptive velocity control for dynamic physical interaction between robot, human and environment," in *Proc. IEEE 17th Int. Conf. Autom. Sci. Eng. (CASE)*, Aug. 2021, pp. 2299–2306.

[25] A. Valente, G. Pavesi, M. Zamboni, and E. Carpanzano, "Deliberative robotics—A novel interactive control framework enhancing human–robot collaboration," *CIRP Ann.*, vol. 71, no. 1, pp. 21–24, 2022. [Online]. Available: https://www.sciencedirect.com/science/article/pii/S0007850622000452

[26] M. Selvaggio, M. Cognetti, S. Nikolaidis, S. Ivaldi, and B. Siciliano, "Autonomy in physical human–robot interaction: A brief survey," *IEEE Robot. Autom. Lett.*, vol. 6, no. 4, pp. 7989–7996, Oct. 2021.

[27] D. P. Losey, C. G. McDonald, E. Battaglia, and M. K. O'Malley, "A review of intent detection, arbitration, and communication aspects of shared control for physical human–robot interaction," *Appl. Mech. Rev.*, vol. 70, no. 1, Jan. 2018, Art. no. 010804.

[28] P. Franceschi, N. Castaman, S. Ghidoni, and N. Pedrocchi, "Precise robotic manipulation of bulky components," *IEEE Access*, vol. 8, pp. 222476–222485, 2020.

[29] P. Franceschi and N. Castaman, "Combining visual and force feedback for the precise robotic manipulation of bulky components," *Proc. SPIE*, vol. 11785, Jun. 2021, Art. no. 1178510, doi: 10.1117/12.2595613.

[30] D. Bazzi, G. Priora, A. M. Zanchettin, and P. Rocco, "RRT* and goal-driven variable admittance control for obstacle avoidance in manual guidance applications," *IEEE Robot. Autom. Lett.*, vol. 7, no. 2, pp. 1920–1927, Apr. 2022.

[31] G. Nicola, E. Villagrossi, and N. Pedrocchi, "Human–robot co-manipulation of soft materials: Enable a robot manual guidance using a depth map feedback," in *Proc. 31st IEEE Int. Conf. Robot Human Interact. Commun. (RO-MAN)*, Aug. 2022, pp. 498–504.

[32] D. Sirintuna, A. Giammarino, and A. Ajoudani, "An object deformation-agnostic framework for human–robot collaborative transportation," *IEEE Trans. Autom. Sci. Eng.*, early access, Mar. 24, 2023, doi: 10.1109/TASE.2023.3259162.

[33] J. Kim, H. Ladjal, D. Folio, A. Ferreira, and J. Kim, "Evaluation of telerobotic shared control strategy for efficient single-cell manipulation," *IEEE Trans. Autom. Sci. Eng.*, vol. 9, no. 2, pp. 402–406, Apr. 2012.

[34] D. Nicolis, M. Palumbo, A. M. Zanchettin, and P. Rocco, "Occlusion-free visual servoing for the shared autonomy teleoperation of dual-arm robots," *IEEE Robot. Autom. Lett.*, vol. 3, no. 2, pp. 796–803, Apr. 2018.

[35] Y. Xu, H. Zhang, L. Cao, X. Shu, and D. Zhang, "A shared control strategy for reach and grasp of multiple objects using robot vision and noninvasive brain–computer interface," *IEEE Trans. Autom. Sci. Eng.*, vol. 19, no. 1, pp. 360–372, Jan. 2022.

[36] K. Kronander and A. Billard, "Stability considerations for variable impedance control," *IEEE Trans. Robot.*, vol. 32, no. 5, pp. 1298–1305, Oct. 2016.

[37] L. Bascetta, "A passivity-based adaptive admittance control strategy for physical human–robot interaction in hands-on tasks," in *Proc. IEEE 18th Int. Conf. Autom. Sci. Eng. (CASE)*, Aug. 2022, pp. 2267–2272.

[38] C. Mu, K. Wang, and Z. Ni, "Adaptive learning and sampled-control for nonlinear game systems using dynamic event-triggering strategy," *IEEE Trans. Neural Netw. Learn. Syst.*, vol. 33, no. 9, pp. 4437–4450, Sep. 2022.

[39] K. Wang and C. Mu, "Learning-based control with decentralized dynamic event-triggering for vehicle systems," *IEEE Trans. Ind. Informat.*, vol. 19, no. 3, pp. 2629–2639, Mar. 2023.

[40] J. Engwerda, "The regular convex cooperative linear quadratic control problem," *Automatica*, vol. 44, no. 9, pp. 2453–2457, Sep. 2008.

[41] J. Engwerda, "Algorithms for computing Nash equilibria in deterministic LQ games," *Comput. Manage. Sci.*, vol. 4, no. 2, pp. 113–140, Apr. 2007.

[42] X. Na and D. J. Cole, "Linear quadratic game and non-cooperative predictive methods for potential application to modelling driver-AFS interactive steering control," *Vehicle Syst. Dyn.*, vol. 51, no. 2, pp. 165–198, Feb. 2013.

[43] X. Na and D. J. Cole, "Modelling of a human driver's interaction with vehicle automated steering using cooperative game theory," *IEEE/CAA J. Autom. Sinica*, vol. 6, no. 5, pp. 1095–1107, Sep. 2019.

[44] X. Na and D. J. Cole, "Game-theoretic modeling of the steering interaction between a human driver and a vehicle collision avoidance controller," *IEEE Trans. Hum.-Mach. Syst.*, vol. 45, no. 1, pp. 25–38, Feb. 2015.

[45] A. Ji and D. Levinson, "A review of game theory models of lane changing," *Transportmetrica A, Transp. Sci.*, vol. 16, no. 3, pp. 1628–1647, Jan. 2020.

[46] X. Na and D. J. Cole, "Experimental evaluation of a game-theoretic human driver steering control model," *IEEE Trans. Cybern.*, vol. 53, no. 8, pp. 4791–4804, Aug. 2023.

[47] X. Na and D. Cole, "Theoretical and experimental investigation of driver noncooperative-game steering control behavior," *IEEE/CAA J. Autom. Sinica*, vol. 8, no. 1, pp. 189–205, Jan. 2021.

[48] J. Inga, M. Flad, and S. Hohmann, "Validation of a human cooperative steering behavior model based on differential games," in *Proc. IEEE Int. Conf. Syst., Man Cybern. (SMC)*, Oct. 2019, pp. 3124–3129.

[49] D. A. Braun, P. A. Ortega, and D. M. Wolpert, "Nash equilibria in multi-agent motor interactions," *PLoS Comput. Biol.*, vol. 5, no. 8, 2009, Art. no. e1000468.

[50] C. Lindig-León, G. Schmid, and D. A. Braun, "Nash equilibria in human sensorimotor interactions explained by Q-learning with intrinsic costs," *Sci. Rep.*, vol. 11, no. 1, pp. 1–15, Oct. 2021.

[51] A. Takagi, G. Ganesh, T. Yoshioka, M. Kawato, and E. Burdet, "Physically interacting individuals estimate the partner's goal to enhance their movements," *Nature Hum. Behav.*, vol. 1, no. 3, pp. 1–6, Mar. 2017.

[52] Y. Li, K. P. Tee, W. L. Chan, R. Yan, Y. Chua, and D. K. Limbu, "Continuous role adaptation for human–robot shared control," *IEEE Trans. Robot.*, vol. 31, no. 3, pp. 672–681, Jun. 2015.

[53] W. Bi, X. Wu, Y. Liu, and Z. Li, "Role adaptation and force, impedance learning for physical human–robot interaction," in *Proc. IEEE 4th Int. Conf. Adv. Robot. Mechatronics (ICARM)*, Jul. 2019, pp. 111–117.

[54] Y. Li, K. P. Tee, R. Yan, W. L. Chan, Y. Wu, and D. K. Limbu, "Adaptive optimal control for coordination in physical human–robot interaction," in *Proc. IEEE/RSJ Int. Conf. Intell. Robots Syst. (IROS)*, Sep. 2015, pp. 20–25.

[55] Y. Li, K. P. Tee, R. Yan, W. L. Chan, and Y. Wu, "A framework of human–robot coordination based on game theory and policy iteration," *IEEE Trans. Robot.*, vol. 32, no. 6, pp. 1408–1418, Dec. 2016.

[56] Y. Li, G. Carboni, F. Gonzalez, D. Campolo, and E. Burdet, "Differential game theory for versatile physical human–robot interaction," *Nature Mach. Intell.*, vol. 1, no. 1, pp. 36–43, Jan. 2019.

[57] R. Zou, Y. Liu, J. Zhao, and H. Cai, "A framework for human–robot-human physical interaction based on N-player game theory," *Sensors*, vol. 20, no. 17, p. 5005, Sep. 2020. [Online]. Available: https://www.mdpi.com/1424-8220/20/17/5005

[58] S. Musić and S. Hirche, "Haptic shared control for human–robot collaboration: A game-theoretical approach," *IFAC-PapersOnLine*, vol. 53, no. 2, pp. 10216–10222, 2020.

[59] P. Franceschi, N. Pedrocchi, and M. Beschi, "Adaptive impedance controller for human–robot arbitration based on cooperative differential game theory," in *Proc. Int. Conf. Robot. Autom. (ICRA)*, May 2022, pp. 7881–7887.

[60] A. Mörtl, M. Lawitzky, A. Kucukyilmaz, M. Sezgin, C. Basdogan, and S. Hirche, "The role of roles: Physical cooperation between humans and robots," *Int. J. Robot. Res.*, vol. 31, no. 13, pp. 1656–1674, Nov. 2012, doi: 10.1177/0278364912455366.

[61] W. Lu, Z. Hu, and J. Pan, "Human–robot collaboration using variable admittance control and human intention prediction," in *Proc. IEEE 16th Int. Conf. Autom. Sci. Eng. (CASE)*, Aug. 2020, pp. 1116–1121.

[62] S. Li, M. Bowman, and X. Zhang, "A general arbitration model for robust human–robot shared control with multi-source uncertainty modeling," 2020, arXiv:2003.05097.

[63] A. Cherubini, R. Passama, A. Crosnier, A. Lasnier, and P. Fraisse, "Collaborative manufacturing with physical human–robot interaction," *Robot. Comput.-Integr. Manuf.*, vol. 40, pp. 1–13, Aug. 2016.

[64] X. Xing, K. Maqsood, D. Huang, C. Yang, and Y. Li, "Iterative learning-based robotic controller with prescribed human–robot interaction force," *IEEE Trans. Autom. Sci. Eng.*, vol. 19, no. 4, pp. 3395–3408, Oct. 2022.

[65] M. Mujica, M. Crespo, M. Benoussaad, S. Junco, and J.-Y. Fourquet, "Robust variable admittance control for human–robot co-manipulation of objects with unknown load," *Robot. Comput.-Integr. Manuf.*, vol. 79, Feb. 2023, Art. no. 102408.

[66] M. Li, H. Cao, X. Song, Y. Huang, J. Wang, and Z. Huang, "Shared control driver assistance system based on driving intention and situation assessment," *IEEE Trans. Ind. Informat.*, vol. 14, no. 11, pp. 4982–4994, Nov. 2018.

[67] Z. Ji et al., "Towards shared autonomy framework for human-aware motion planning in industrial human–robot collaboration," in *Proc. IEEE 16th Int. Conf. Autom. Sci. Eng. (CASE)*, Aug. 2020, pp. 411–417.

[68] S. Ko and R. Langari, "Shared control between human driver and automation in cooperative driving based on game theoretic model predictive control," in *Proc. Dyn. Syst. Control Conf.*, vol. 59162, 2019, Art. no. V003T18A004.

[69] S. Ko and R. Langari, "Shared control between human driver and machine based on game theoretical model predictive control framework," in *Proc. IEEE/ASME Int. Conf. Adv. Intell. Mechatronics (AIM)*, Jul. 2020, pp. 649–654.

[70] B. Siciliano and L. Villani, *Robot Force Control*. Berlin, Germany: Springer, 1999.

[71] T. Basar and G. J. Olsder, *Dynamic Noncooperative Game Theory*, 2nd ed. Philadelphia, PA, USA: Society for Industrial and Applied Mathematics, 1998.

[72] J. Engwerda, *LQ Dynamic Optimization and Differential Games*. Hoboken, NJ, USA: Wiley, 2005.

[73] S. Cremer, S. K. Das, I. B. Wijayasinghe, D. O. Popa, and F. L. Lewis, "Model-free online neuroadaptive controller with intent estimation for physical human–robot interaction," *IEEE Trans. Robot.*, vol. 36, no. 1, pp. 240–253, Feb. 2020.

This article has been accepted for inclusion in a future issue of this journal. Content is final as presented, with the exception of pagination.

16   IEEE TRANSACTIONS ON AUTOMATION SCIENCE AND ENGINEERING

[74] Y. Li, J. Eden, G. Carboni, and E. Burdet, "Improving tracking through human–robot sensory augmentation," *IEEE Robot. Autom. Lett.*, vol. 5, no. 3, pp. 4399–4406, Jul. 2020.

[75] P. Leica, F. Roberti, M. Monllor, J. M. Toibero, and R. Carelli, "Control of bidirectional physical human–robot interaction based on the human intention," *Intell. Service Robot.*, vol. 10, no. 1, pp. 31–40, Jan. 2017.

[76] P. Franceschi, F. Bertini, F. Braghin, L. Roveda, N. Pedrocchi, and M. Beschi, "Predicting human motion intention for pHRI assistive control," 2023, *arXiv:2307.10743*.

[77] J. A. Saunders and D. C. Knill, "Humans use continuous visual feedback from the hand to control fast reaching movements," *Exp. Brain Res.*, vol. 152, no. 3, pp. 341–352, Oct. 2003.

[78] J. Inga, M. Eitel, M. Flad, and S. Hohmann, "Evaluating human behavior in manual and shared control via inverse optimization," in *Proc. IEEE Int. Conf. Syst., Man, Cybern. (SMC)*, Oct. 2018, pp. 2699–2704.

[79] P. Franceschi, N. Pedrocchi, and M. Beschi, "Inverse optimal control for the identification of human objective: A preparatory study for physical human–robot interaction," in *Proc. IEEE 27th Int. Conf. Emerg. Technol. Factory Autom. (ETFA)*, Sep. 2022, pp. 1–6.

[80] J. F. Nash, "The bargaining problem," *Econometrica*, vol. 18, no. 2, pp. 155–162, Jan. 1950. [Online]. Available: http://www.jstor.org/stable/1907266

[81] E. Kalai and M. Smorodinsky, "Other solutions to Nash's bargaining problem," *Econometrica, J. Econ. Soc.*, vol. 43, pp. 513–518, May 1975.

[82] E. Kalai, "Proportional solutions to bargaining situations: Interpersonal utility comparisons," *Econometrica, J. Econ. Soc.*, vol. 45, pp. 1623–1630, Oct. 1977.

[83] P. Franceschi, S. Mutti, and N. Pedrocchi, "Optimal design of robotic work-cell through hierarchical manipulability maximization," *Robot. Comput.-Integr. Manuf.*, vol. 78, Dec. 2022, Art. no. 102401.

[84] M. J. Tsai and Y. H. Chiou, "Manipulability of manipulators," *Mechanism Mach. Theory*, vol. 25, no. 5, pp. 575–585, Jan. 1990.

[85] *Robots and Robotic Devices—Safety Requirements for Industrial Robots—Part 1: Robots*, International Organization for Standardization, Geneva, Switzerland, Standard ISO 10218-1:2011, 2011.

[86] *Robots and Robotic Devices—Safety Requirements for Industrial Robots—Part 2: Robot Systems and Integration*, International Organization for Standardization, Geneva, Switzerland, Standard ISO 10218-2:2011, 2011.

[87] *Robots and Robotic Devices—Collaborative Robots*, International Organization for Standardization, Geneva, Switzerland, Standard ISO/TS 15066:2016, 2016.

[88] B. Lacevic, A. M. Zanchettin, and P. Rocco, "Safe human–robot collaboration via collision checking and explicit representation of danger zones," *IEEE Trans. Autom. Sci. Eng.*, vol. 20, no. 2, pp. 846–861, Apr. 2023.

[89] P. Franceschi, M. Beschi, N. Pedrocchi, and A. Valente, "Modeling and analysis of pHRI with differential game theory," 2023, *arXiv:2307.10739*.

[90] H.-N. Wu, "Online learning human behavior for a class of human-in-the-loop systems via adaptive inverse optimal control," *IEEE Trans. Hum.-Mach. Syst.*, vol. 52, no. 5, pp. 1004–1014, Oct. 2022.

[91] W. Jin, D. Kulic, J. F. Lin, S. Mou, and S. Hirche, "Inverse optimal control for multiphase cost functions," *IEEE Trans. Robot.*, vol. 35, no. 6, pp. 1387–1398, Dec. 2019.

[92] J. Inga, A. Creutz, and S. Hohmann, "Online inverse linear-quadratic differential games applied to human behavior identification in shared control," in *Proc. Eur. Control Conf. (ECC)*, Jun. 2021, pp. 353–360.

[93] P. Franceschi, N. Pedrocchi, and M. Beschi, "Identification of human control law during physical human–robot interaction," *Mechatronics*, vol. 92, Jun. 2023, Art. no. 102986. [Online]. Available: https://www.sciencedirect.com/science/article/pii/S0957415823000429

[94] P. Franceschi, M. Maccarini, D. Piga, M. Beschi, and L. Roveda, "Human preferences' optimization in pHRI collaborative tasks," in *Proc. 20th Int. Conf. Ubiquitous Robots (UR)*, Jun. 2023, pp. 693–699.

Paolo Franceschi received the B.S. degree in aerospace engineering and the M.S. degree in mechanical engineering from Politecnico of Milano, in 2015 and 2017, respectively. He is currently pursuing the Ph.D. degree with the University of Brescia. From 2016 to 2017, he was a Visiting Scholar with the IBM Almaden Research Center, San Jos, CA, USA, to complete the master's thesis on modeling and controlling a bipedal robot. In 2018, he joined STIIMA-CNR, Milan, Italy, as a Research Fellow. From 2022 to 2023, he was a Visiting Ph.D. Student with Istituto Dalle Molle sull' Intelligenza Artificiale (IDSIA), Lugano, Switzerland. Since October 2023, he has been a Researcher with the Department of Innovative Technologies, University of Applied Science and Arts of Southern Switzerland (SUPSI), Lugano. His research interests include human–robot interaction, interaction control for robotic manipulators, and optimization of complex robotics manipulation working area and tasks.

Nicola Pedrocchi received the M.S. degree in mechanical engineering from the University of Brescia, Brescia, Italy, in 2004, and the Ph.D. degree in applied mechanics and robotics in 2008. From 2008 to 2011, he was a Research Assistant with the Institute of Industrial Technologies and Automation, National Research Council of Italy, where he has been a Full Researcher, since 2011. Since 2015, he has been coordinating the activity of the Robot Motion Control and Robotized Processes Laboratory, CNR-STIIMA. He has involved in research for accurate elastic modeling and dynamic calibration of industrial robots. His research interests include control techniques for industrial manipulators in advanced applications requiring the interaction of robots and environment, such as technological tasks, robots and human operators, such as workspace sharing and teach-by-demonstration.

Manuel Beschi (Member, IEEE) received the bachelor's and master's degrees in industrial automation engineering from the University of Brescia, Brescia, Italy, in 2008 and 2010, respectively, and the Ph.D. degree in computer science, engineering, and control systems technologies from the Department of Mechanical and Industrial Engineering. He is currently an Assistant Professor with the University of Brescia.